

MicroRNA hsa-miR-150-5p inhibits nasopharyngeal carcinogenesis by suppressing PYCR1 (pyrroline-5-carboxylate reductase 1)

Zhiqun Li*, Xiaoliu Zhou*, Jiajun Huang, Zhencai Xu, Chengliang Xing, Junwei Yang, and Xuejun Zhou

Department of Otolaryngology Head and Neck Surgery, The First Affiliated Hospital of Hainan Medical University, Haikou, China

ABSTRACT

Nasopharyngeal cancer is a rare cancer type, but with a low five-year survival rate. Dysregulation of pyrroline-5-carboxylate reductase 1 (PYCR1) and microRNA hsa-miR-150-5p is involved in the development of various cancers. However, the molecular mechanism of the hsa-miR-150-5p-PYCR1 axis in nasopharyngeal cancer remains unclear. To identify the mechanism of the hsa-miR-150-5p-PYCR1 axis, the expression of hsa-miR-150-5p and PYCR1 in nasopharyngeal cancer tissues and cells was first measured by reverse transcription quantitative polymerase chain reaction. The luciferase and RNA pull-down assays were used to confirm the interaction between hsa-miR-150-5p and PYCR1. The overexpression of hsa-miR-150-5p and PYCR1 was detected by cell viability, proliferation, western blotting, migration, and invasion in nasopharyngeal cancer cells. The expression levels of hsa-miR-150-5p was reduced in the nasopharyngeal cancer tissues and cells and were negatively correlated with the PYCR1 levels. The upregulation of hsa-miR-150-5p significantly repressed cell growth and promoted apoptosis. However, the upregulation of PYCR1 expression significantly promoted nasopharyngeal carcinogenesis, which could abolish the inhibitory effect of hsa-miR-150-5p. In conclusion, we clarified that hsa-miR-150-5p attenuated nasopharyngeal carcinogenesis by reducing the PYCR1 expression levels. This provides a new perspective of nasopharyngeal cancer involving both hsa-miR-150-5p and PYCR1 for the treatment of nasopharyngeal cancer.

ARTICLE HISTORY

Received 21 July 2021
Revised 12 October 2021
Accepted 13 October 2021

KEYWORDS

Hsa-miR-150-5p; PYCR1;
nasopharyngeal cancer

Introduction

Nasopharyngeal cancer (NPC) is highly prevalent in northern Africa and south-eastern Asia, especially in southeastern China [1]. Radiotherapy, chemotherapy, or combination treatments are common strategies that are used to treat patients with NPC. Unfortunately, a low five-year survival rate remains a serious problem [2]. Many studies have suggested the dysregulation of cell growth and apoptosis of NPC cells [3,4]; however, the potential mechanism of the pathogenesis of NPC needs to be elucidated.

MicroRNAs (miRNAs) are a variety of non-coding RNAs consisting of 19–24 nucleotides, that regulate cellular biological processes by binding to the target gene 3 untranslated regions (UTRs) [5]. A growing body of evidence indicates that these miRNAs play key roles in carcinogenesis, namely cell growth, differentiation, and

apoptosis [6,7]. Hsa-miR-150-5p participates in the regulation of various cancers, including breast cancer, colorectal cancer, and oral squamous cell carcinoma (OSCC) [8–10]. For instance, hsa-miR-150-5p expression was dramatically decreased in OSCC tissues, which further repressed cell growth and enhanced apoptosis of OSCC cells [10]. Additionally, hsa-miR-150-5p expression is down-regulated in breast cancer tissues and attenuates the proliferation and migration of breast cancer cells [8]. Notably, hsa-miR-150-5p has also been associated with NPC development [11–14]. Studies have reported that hsa-miR-150-5p hampers the NPC cell migration by reducing CD44 molecule (CD44) expression [11]. High levels of hsa-miR-150-5p inhibiting glycogen synthase kinase 3 beta (GSK3 β) protein levels have contributed to poor prognosis in NPC patients [12]. In addition, Zhu et al. [14] found that hsa-miR-150-5p

CONTACT Xuejun Zhou  xuejunzhou65@163.com  Department of Otolaryngology Head and Neck Surgery, The First Affiliated Hospital of Hainan Medical University, No. 31 Longhua Road, Longhua District, Haikou, Hainan 570102, China

*These authors contributed equally to this work.

 Supplemental data for this article can be accessed [here](#).

© 2021 The Author(s). Published by Informa UK Limited, trading as Taylor & Francis Group.
This is an Open Access article distributed under the terms of the Creative Commons Attribution License (<http://creativecommons.org/licenses/by/4.0/>), which permits unrestricted use, distribution, and reproduction in any medium, provided the original work is properly cited.

expression was significantly decreased in NPC, and its knockdown promoted the proliferation, migration, and invasion of NPC cells. However, whether hsa-miR-150-5p plays a role in *PYCR1* expression (pyrroline-5-carboxylate reductase 1) remains unclear.

PYCR1 encodes an enzyme that catalyzes the last step of proline synthesis, which plays a key role as an oncogene in cancer progression [15–17]. For instance, the downregulation of *PYCR1* inhibited the growth of lung adenocarcinoma cells by repressing the Janus kinase (JAK)-signal transducer and activator of transcription-3 (STAT3) signaling pathway [15]. Wang et al. reported that *PYCR1* enhanced non-small-cell lung cancer (NSCC) cell growth when miR-488 was downregulated [16]. Another study also indicated that the downregulation of *PYCR1* significantly suppressed prostate cancer cell growth and colony formation, but enhanced cell apoptosis [17]. However, the effect of *PYCR1* on NPC cells remains unknown.

In this study, we sought to elucidate the regulatory mechanism of hsa-miR-150-5p-*PYCR1* in NPC. We hypothesized that hsa-miR-150-5p might hamper cell growth during NPC development by repressing *PYCR1* expression. Our study may provide a good potential therapeutic approach for the clinical treatment of patients with NPC.

Methods

Tumor specimens and cell lines

Tumor tissues and adjacent normal tissues (>5 cm away from the tumor margin) were collected from patients with NPC (n = 38) between January 2020 and January 2021 from our hospital with informed consent. The clinical baseline characteristics of the patients with NPC are shown in Supplementary Table S1. Informed consent was obtained from all individuals, and the research protocol was approved by the Ethics Committee of The First Affiliated Hospital of Hainan Medical University (Approval no. KY2019012). Normal human nasopharyngeal epithelial (NP69) and NPC cells (TW03, C666-1, and SUNE-1) were obtained from the American Type Culture Collection (Manassas, VA, USA). Cells were maintained in

RPMI-1640 medium (Gibco, USA) containing 10% fetal bovine serum (FBS) (Gibco, USA) in a cell incubator at 37°C and 5% CO₂.

Reverse transcription quantitative polymerase chain reaction (RT-qPCR)

The total RNA from the tissues and cells was extracted using Trizol (Invitrogen, USA) and was reverse transcribed using a cDNA Reverse Transcription Kit (Liankebio, China). SYBR Premix Ex Taq (Takara, Japan) was used to detect *PYCR1* expression. Tissue and cell miRNAs were extracted using an miRNA Isolation Kit (Thermo Fisher, USA) and reverse transcribed using the TaqMan MicroRNA Reverse Transcription Kit (Thermo Fisher, USA). The TaqMan OpenArray Real-Time PCR Master Mix (Thermo Fisher, USA) was used to detect hsa-miR-150-5p expression. The expression of *PYCR1* and hsa-miR-150-5p was normalized to glyceraldehyde-3-phosphate dehydrogenase (GAPDH) and Uracil6 (U6), respectively, using the 2^{-ΔΔCt} method [18]. The primers used are listed in Table 1.

Cell transfection

All transfectants, including *PYCR1* overexpression plasmid and empty vector, hsa-miR-150-5p mimic, and mimic negative control (NC) were purchased from Thermo Fisher (USA). Before subsequent functional experiments, C666-1 and SUNE-1 cells were transfected with the Lipo3000 (Invitrogen, USA) for 48 h.

Cell counting kit-8 (CCK-8) detection

The transfected C666-1 and SUNE-1 cells (5 × 10³) were seeded into 96-well plates and examined using

Table 1. Sequence of PCR primers used in this study.

Gene name	Primer type	Sequence
miR-150-5p	Forward	5'-TCGGCGTCTCCCAACCCTTGAC-3'
	Reverse	5'-GTCGTATCCAGTGCAGGGTCCGAGGT-3'
CSE1L	Forward	5'-TGACCAA-CACTCCAGTCGTG-3'
	Reverse	5'-GTCCAGCTTCACCTTGCCA-3'
GAPDH	Forward	5'-GGAGCGAGATCCCTCCAAAAT-3'
	Reverse	5'-GGCT-GTTGTCATACTTCTCATGG-3'
U6	Forward	5'-CTCGTTCGGCAGCACATATACT-3'
	Reverse	5'-ACGCTTACGAATTTGCGTGTC-3'

the CCK-8 kit (Cat#: K1018; APEXBIO, China) according to the previous study [19]. At 0, 24, 48, and 72 h, 10 μ L CCK-8 buffer was added to the plates and incubated for another 2 h. Finally, the optical density at 450 nm (OD_{450}) was obtained using a multimode plate reader (Thermo Fisher, USA).

5'-Bromo-2'-deoxyuridine (BrdU) detection

The transfected C666-1 and SUNE-1 cells (2×10^4) were seeded into 96-well plates. At 70% confluence, the cells were washed twice, and BrdU (Cat#: 6813, CST, USA) labeling solution was added to the cells. After 6 h of incubation, the cells were washed twice, fixed, and denatured by the fixation/denaturation solution. The BrdU antibody was then added and the cells were incubated for 2 h. Next, the cells were washed twice, and the secondary horse radish peroxidase (HRP)-mouse antibody was used for another 2 h of incubation. Finally, the cells were washed twice and HRP substrate TMB was added to the cells, and the OD_{450} was obtained on a multimode-plate-reader (Thermo Fisher, USA) [20].

Wound healing detection

The transfected C666-1 and SUNE-1 cells (1×10^6) were seeded into 6-well plates. After the cells reached 70% confluence, the diameter through the plate was drawn using a sterile pipette, and the floating cells were washed away. At 0 and 24 h, images of the scratches were obtained using a light microscope and recorded [21].

Cell invasion detection

Matrigel (Corning, USA) was added into the transwell chamber with 8- μ m pore (Cat#: #3244, Corning, USA). RPMI-1640 medium containing 10% FBS was added to the lower chambers. The transfected C666-1 and SUNE-1 cells were seeded into the upper chamber. After 48 h, the invaded cells were fixed with 4% paraformaldehyde, washed twice with PBS, and stained with 0.1% crystal violet. Subsequently, the invaded cells were imaged under a microscope (Olympus, Japan) [22].

Luciferase detection

The pmiRGLO plasmid containing PYCR1 3'-UTRs wild-type (WT) or mutant (MUT) sequences was provided by Tuoran Co., Ltd (Shanghai, China). C666-1 and SUNE-1 cells (5×10^5) were seeded into 24-well plates, and the cells were transfected with the plasmids, and either miR-NC or hsa-miR-150-5p using Lipo3000. After 48 h, firefly and Renilla luciferase activities were examined using the Luciferase Assay Kit (RG027, Beyotime, China). Renilla luciferase activity was used as an internal control [23].

RNA-pull down analysis

Biotin-labeled miR-185-5p (Bio-miR-185-5p) and miR-185-5p negative control (Bio-NC), were obtained from Thermo Fisher (USA). The cell lysate suspension was mixed with Bio-hsa-miR-150-5p or Bio-NC and incubated with streptavidin beads (Cat#: #88,817, Thermo Fisher, USA) at 4°C overnight. Subsequently, the eluted solution was collected and purified using a kit (DP412, Tiangen, China). PYCR1 expression was detected by RT-qPCR [24].

RNA immunoprecipitation (RIP) assay

The EZ-Magna RIP Kit (Millipore, Bedford, MA, USA) was used for the RIP assay, as per the manufacturer's protocol. In brief, C666-1 and SUNE-1 cells were lysed with RIP lysis buffer. The cell extracts were then co-incubated with RIP buffer containing magnetic beads coupled to a human anti-Ago2 antibody (Millipore) or IgG, and then mixed with protease K to digest proteins. The immunoprecipitated RNA was isolated, purified, and analyzed using western blotting [25].

Western blot analysis

Proteins from the transfected C666-1 and SUNE-1 cells were obtained using radioimmunoprecipitation assay (RIPA) buffer (P0013 C, Beyotime, China). The 20 μ g per well protein sample was loaded onto 10% sulfate-polyacrylamide gel electrophoresis (SDS-PAGE) and transferred to polyvinylidene fluoride (PVDF) membranes. After blocking with 5% bovine serum albumin, anti-

PYCR1 (Cat#: 47935S, CST, USA), anti-Bax (Cat#: ab32503, Abcam, UK), Anti- Bcl-2 (Cat#: ab32124, Abcam, UK), and anti-GAPDH (Cat#: 5714, CST, USA) diluted 1:1,000 were used to incubate the membranes overnight at 4°C. Subsequently, anti-HRP-Rabbit (Cat#: 7074, CST, USA) was used to incubate the membranes for 1 h. Electrogenerated chemiluminescence (ECL) reagents (P0018S, Beyotime, China) were used to develop the protein bands. GAPDH protein level was used as an internal control [26].

Statistical analysis

The paired *t*-test, one-way analysis of variance (ANOVA), and two-way ANOVA were used to compare two groups and multiple groups, respectively, using GraphPad 8.0 (GraphPad, USA). The correlation between hsa-miR-150-5p and PYCR1 in NPC tissues was analyzed using Spearman's correlation analysis. Data are shown as mean \pm standard deviation (SD) from triplicate experiments. Statistical significance was set at $P < 0.05$.

Results

In this study, we aimed to explore the role of hsa-miR-150-5p-PYCR1 in NPC. We conducted a series of in vitro experiments and found that hsa-miR-150-5p inhibited the activity, proliferation, migration, and invasion, as well as promoted apoptosis of NPC by negatively regulating PYCR1. Our data are the first to investigate the function and clinical expression of hsa-miR-150-5p-PYCR1 in NPC, providing new insights into the pathogenesis of NPC.

PYCR1 and hsa-miR-150-5p were identified to be potential participants in NPC

We first analyzed the mRNA profiling of GSE64634, and the results showed that five genes were conspicuously increased in NPC with the criteria of adjusted $P < 0.05$, and $\log_{2}FC \geq 1.5$ (Figure 1a). We investigated the GEPIA database for expression in head and neck squamous cell carcinoma. Among the five genes, *SAC3D1* and *PYCR1* were also significantly upregulated in the GEPIA HNSC data (Figure 1b–f). Therefore, the

expression of *SAC3D1* and *PYCR1* in clinical tissues was detected by RT-qPCR. RT-qPCR showed that both *SAC3D1* and *PYCR1* levels were increased in NPC tissues, but *PYCR1* was upregulated (Figure 1g). In addition, we noticed that *PYCR1* has been reported to be a significant cancer driver and its silencing could significantly suppress carcinogenesis and progression [15–17,27–29]. Nonetheless, the functions of *PYCR1* in nasopharyngeal cancer have not been studied. We speculated that *PYCR1* could be a cancer driver in NPC. Thus, we selected *PYCR1* as the study object. To identify an upstream miRNA regulator of *PYCR1* in NPC, we analyzed the miRNA profiling of GSE118613, and the results showed that 17 miRNAs were significantly downregulated in NPC with $\text{adj.}P < 0.05$, and $\log_{2}FC < -1.5$ (Supplementary Table S1). By intersecting the 17- miRNA list with the predicted target miRNAs of *PYCR1* by TargetsScan (Supplementary Table 2), hsa-miR-150-5p was identified (Figure 1h). It has been reported that hsa-miR-150-5p could be a potent carcinogen inhibitor in NPC [13]. Thus, we aimed to study the biological roles of hsa-miR-150-5p and *PYCR1* in NPC cell phenotypes.

Hsa-miR-150-5p suppressed NPC cell progression

To clarify the effect of hsa-miR-150-5p in NPC, we analyzed NPC tissues and hsa-miR-150-5p expression. We found that hsa-miR-150-5p expression was significantly repressed by 50% in the NPC tissue samples, and the TW03, C666-1, and SUNE-1 NPC cells showed a notable decrease in the hsa-miR-150-5p expression levels compared with normal cells (Figures 2a,b). We performed further studies in C666-1 and SUNE-1 cell lines as these indicated the lowest hsa-miR-150-5p expression in the cells. Next, we transfected hsa-miR-150-5p mimics and NC into the C666-1 and SUNE-1 cells. The results illustrated that the mimic groups in the C666-1 and SUNE-1 cells were enhanced by approximately an 8-fold and 5-fold hsa-miR-150-5p expression compared with blank cells, respectively (Figure 2c). Additionally, the mimic groups conspicuously attenuated cell viability compared with the blank cells in both cell lines (Figure 2d). Furthermore, the mimics groups decreased cell proliferation by

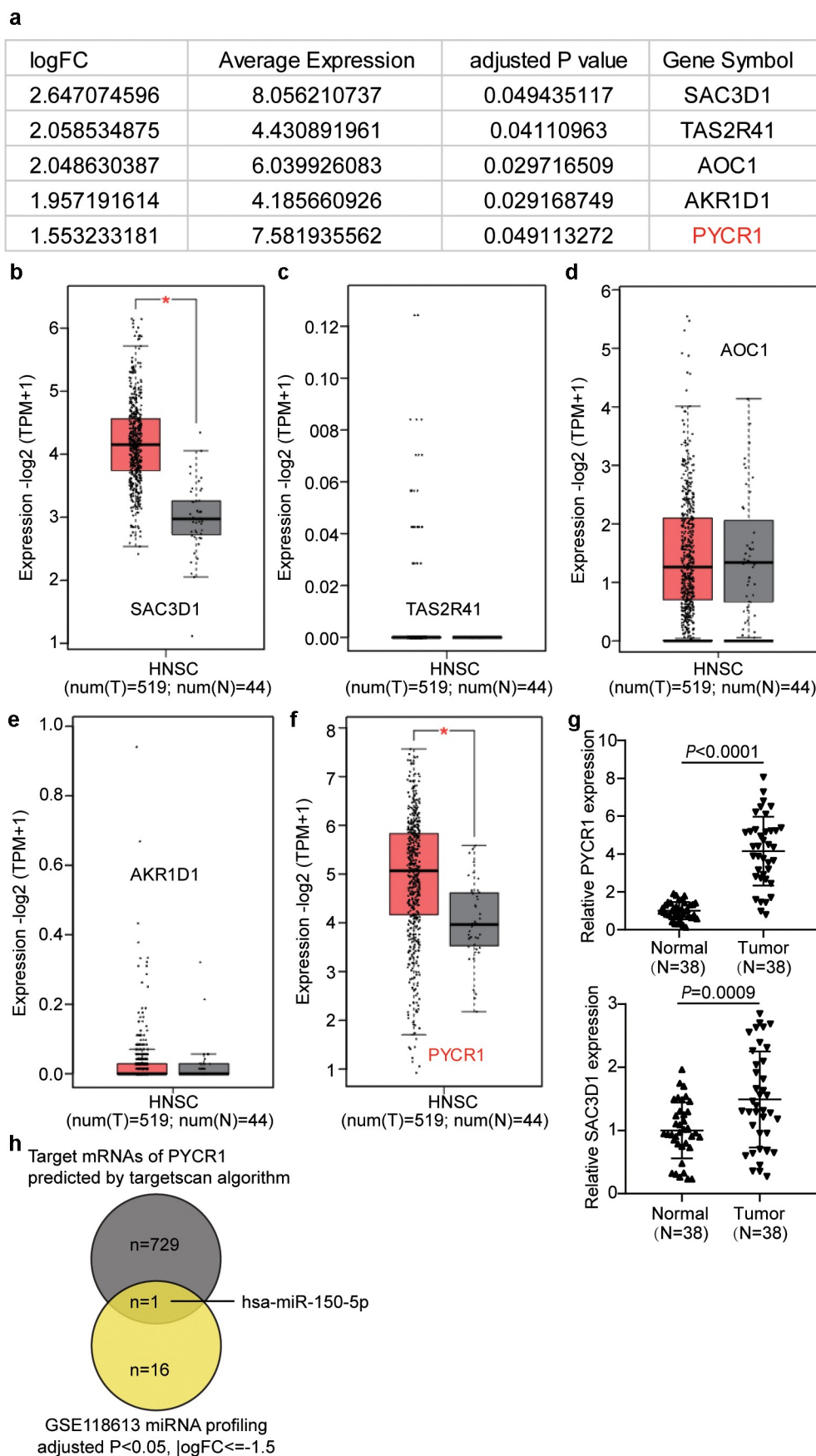


Figure 1. PYCR1 and hsa-miR-150-5p were selected to be studied in this research.

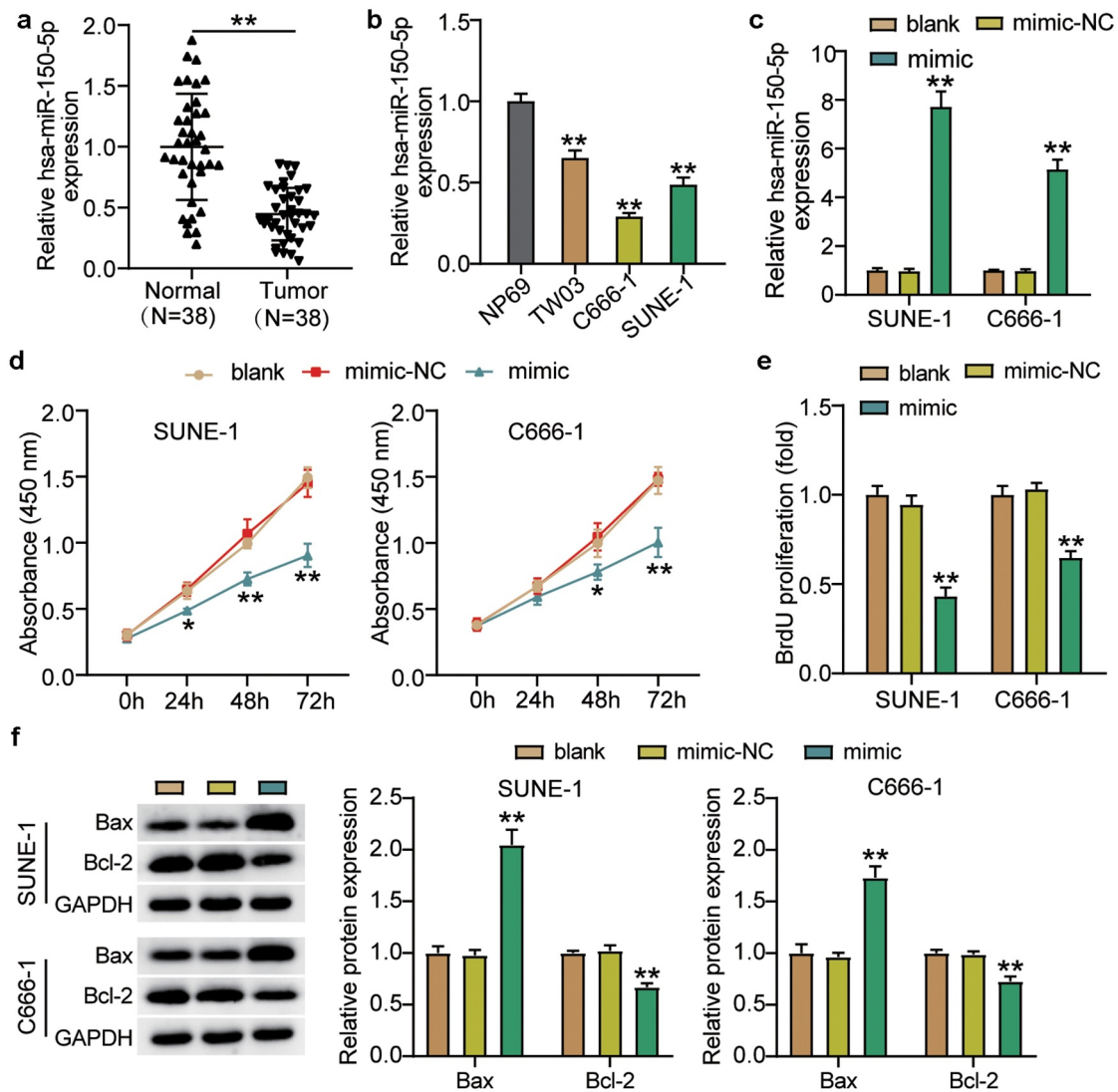


Figure 2. Hsa-miR-150-5p inhibited NPC cells viability and proliferation.

(a) RT-qPCR detection of hsa-miR-150-5p expression in NPC tissues and normal tissues. $n = 38$. **, $P < 0.001$. (b) RT-qPCR detection of hsa-miR-150-5p expression in NPC cells lines (TW03, C666-1 and SUNE-1) and normal cell (NP69). **, $P < 0.001$ compared with NP69. (c) Measurement of hsa-miR-150-5p expression in C666-1 and SUNE-1 cells transfected with mimic-NC and hsa-miR-150-5p mimic by RT-qPCR. (d) Cell viability was detected in C666-1 and SUNE-1 cells transfected with mimic-NC and hsa-miR-150-5p mimic by CCK-8 assay. (e) Cell proliferation was detected in C666-1 and SUNE-1 cells transfected with mimic-NC and hsa-miR-150-5p mimic. (f) Bax and Bcl-2 protein expression was detected in C666-1 and SUNE-1 cells transfected with e mimic-NC and hsa-miR-150-5p mimic by western blot assay. $n = 3$. *, $P < 0.05$; **, $P < 0.001$ compared with blank. NC, negative control; mimic, hsa-miR-150-5p mimic.

approximately 50% compared with blank cells in both cell lines (Figure 2e). In addition, western blotting showed that hsa-miR-150-5p overexpression inhibited the level of BCL-2 protein and upregulated BAX (Figure 2f). Meanwhile, the

mimic groups in C666-1 and SUNE-1 cells showed 50% and 30% cell migration compared with blank cells, respectively (Figure 3a). Moreover, the mimic groups in C666-1 and SUNE-1 cells showed approximately 50% and 30% decrease in the cell

(a) The significantly upregulated genes in NPC in GSE64634 data. Five genes were identified. Selection criteria: adjusted $P < 0.05$, $\log_{2}FC \geq 1.5$. (b–f) The expression of the five genes in GEPIA HNSC data. HNSC: head and neck squamous cell carcinoma. (g) RT-qPCR analysis of SAC3D1 and PYCR1 expression in NPC tissues and normal tissues. $n = 38$. **, $P < 0.001$. (h) The candidate miRNA that both targets PYCR1 mRNA and significantly downregulates in NPC (data from GSE118613 data analysis).

invasion compared with blank cells, respectively (Figure 3b). The data showed that hsa-miR-150-5p attenuated the progression in NPC.

PYCR1 is a target of hsa-miR-150-5p

The binding sequence between PYCR1 and hsa-miR-150-5p is shown in Figure 4a using TargetScan Human 7.2. Next, we transfected plasmids containing PYCR1 3-UTR WT or MUT sequences, and hsa-miR-150-5p-NC or hsa-miR-150-5p-mimic into C666-1 and SUNE-1 cells. The results showed that the luciferase activities of WT +mimic groups were dramatically downregulated by approximately 50%, while the MUT +mimic groups showed no difference in both cells (Figure 4b), which was further verified by RNA-pull down assay (Figure 4c). To further confirm the interaction between PYCR1 and hsa-miR-150-5p, an RIP assay was performed. A prominent enrichment of hsa-miR-150-5p and

PYCR1 was observed in Ago2 (Figure 4d), suggesting that the specificity of the interaction between hsa-miR-150-5p and PYCR1. The C666-1 and SUNE-1 cells showed significantly enhanced PYCR1 expression compared with normal cells (Figure 4e). Additionally, hsa-miR-150-5p was negatively correlated with PYCR1 levels in NPC tumor tissues (Figure 4f). Taken together, these data suggest that hsa-miR-150-5p directly targets PYCR1.

Hsa-miR-150-5p attenuated the development of NPC via repressing PYCR1

To corroborate the role of the hsa-miR-150-5p-PYCR1 axis in NPC, we transfected empty vector +mimic-NC, PYCR1 overexpression (OE), hsa-miR-150-5p mimic, and OE+ mimic into C666-1 and SUNE-1 cells. The results showed a nearly 1.5-fold increase in PYCR1 protein level in the OE groups, while a 50% decrease in PYCR1

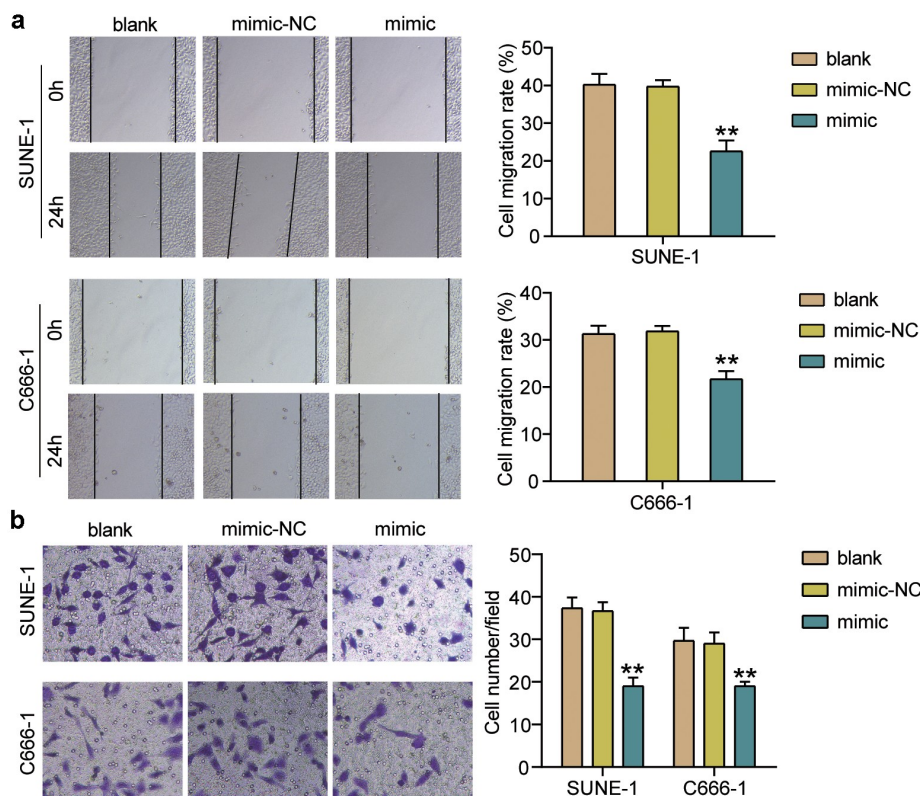


Figure 3. Hsa-miR-150-5p inhibited cell migration and invasion of NPC cells.

(a) Cell migration was detected in C666-1 and SUNE-1 cells transfected with mimic-NC and hsa-miR-150-5p mimic. (b) Cell invasion was detected in C666-1 and SUNE-1 cells transfected with mimic-NC and hsa-miR-150-5p mimic. $n = 3$. **, $P < 0.001$ compared with blank. NC, negative control; mimic, hsa-miR-150-5p mimic.

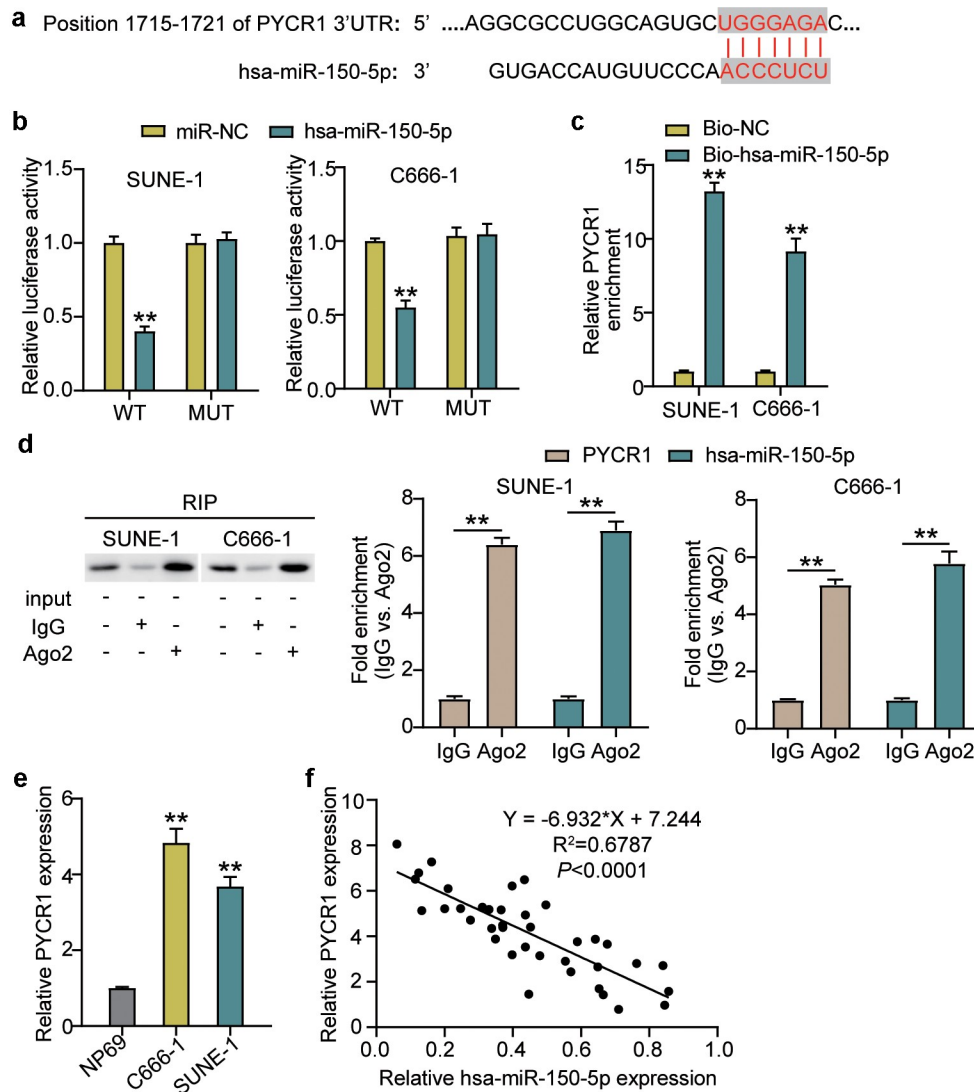


Figure 4. PYCR1 was a target of hsa-miR-150-5p.

(a) Bioinformatics analysis showed the predicted binding sequence of PYCR1 3'-UTR. (b) Dual luciferase assay was performed in cells co-transfected with plasmids PYCR1-WT or PYCR1-MUT and miR-NC or hsa-miR-150-5p mimic in C666-1 and SUNE-1 cells. **, $P < 0.001$ compared with miR-NC. (c) RNA pull-down analysis of PYCR1 expression in C666-1 and SUNE-1 cells. **, $P < 0.001$ compared with Bio-NC. (d) Association of hsa-miR-150-5p and PYCR1 expression levels with AGO2 were determined by RIP-western blotting with AGO2 antibody and RT-qPCR used for RIP analysis as compared with IgG group. **, $P < 0.001$. (e) RT-qPCR detection of expression of PYCR1 in the NPC C666-1 and SUNE-1 cells and NP69 cells. **, $P < 0.001$ compared with NP69. (f) Correlation analysis between the hsa-miR-150-5p expression and expression in the NPC tumor tissues. $n = 3$. WT, wild-type; MUT, mutant; NC, negative control.

protein expression was observed in both C666-1 and SUNE-1 cells. However, the PYCR1 protein level in the OE+ mimic group was comparable to that in the blank group (Figure 5a). Next, the OE groups showed increased cell viability compared with the blank groups, while cells transfected with mimic+ OE counteracted this effect (Figure 5b). In addition, the OE groups showed approximately 1.5-fold upregulated cell

proliferation compared with the blank groups, which was inhibited by the co-transfection with the mimic (Figure 5c). Moreover, the Bcl-2 protein in the OE group was significantly upregulated and Bax was downregulated compared with the blank group, and the effect was reversed by mimic+ OE (Figure 5d). Furthermore, the OE groups displayed a 1.3-fold increase in cell migration compared to the blank groups, whereas the

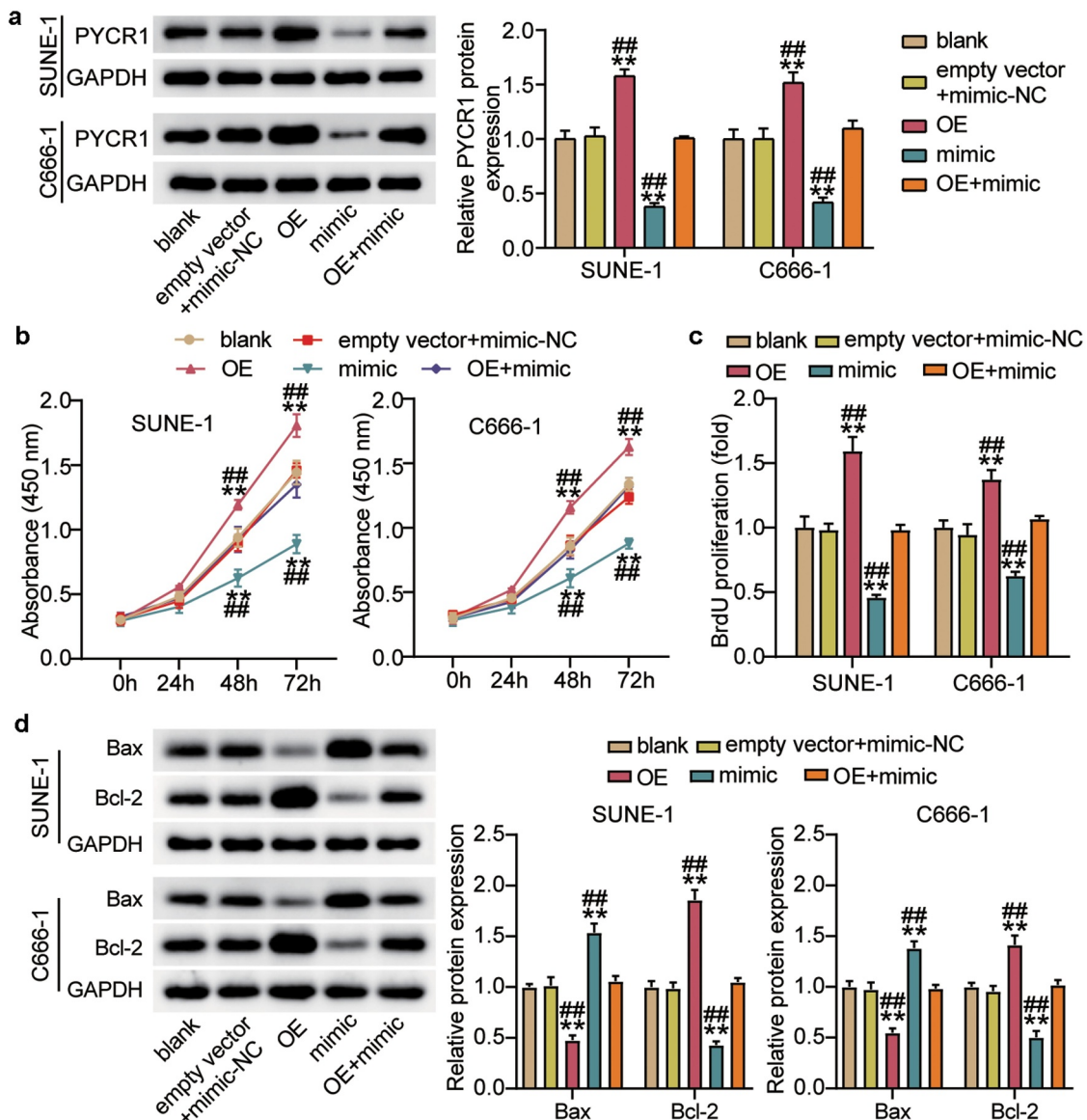


Figure 5. Hsa-miR-150-5p targeting PYCR1 repressed cell proliferation, but enhanced cell apoptosis of NPC cells.

(a) Measurement of PYCR1 protein expression in C666-1 and SUNE-1 cells transfected with empty vector+mimic-NC, OE, mimic and mimic+ OE by western blot. (b) Cell viability was detected in C666-1 and SUNE-1 cells transfected with empty vector+mimic-NC, OE, mimic and mimic+ OE by CCK-8 assay. (c) Cell proliferation was detected in C666-1 and SUNE-1 cells transfected with empty vector+mimic-NC, OE, mimic and mimic+ OE by BrdU assay. (d) Bax and Bcl-2 protein expression was detected in C666-1 and SUNE-1 cells transfected with empty vector+mimic-NC, OE, mimic and mimic+ OE by western blot assay. $n = 3$. *, $P < 0.05$; **, $P < 0.001$ compared with blank. #, $P < 0.05$; ##, $P < 0.001$ compared with mimic+ OE. NC, negative control; mimic, hsa-miR-150-5p mimic; OE, PYCR1 overexpression; mimic+OE, hsa-miR-150-5p mimic+ PYCR1 overexpression.

role was repressed by cells transfected with mimic + OE (Figure 6a). Finally, the OE groups showed a 1.3-fold increase in cell migration compared to the blank groups, but the mimic+ OE treatment suppressed this effect (Figure 6b). Collectively, these results showed that hsa-miR-150-5p attenuated the development of NPC by repressing PYCR1.

Discussion

This study showed that hsa-miR-150-5p levels were downregulated in the NPC tissue samples and cells and were negatively correlated with the PYCR1 levels in the NPC tumor tissue samples. The upregulation of hsa-miR-150-5p inhibits NPC cell progression. Importantly, hsa-miR-150-5p

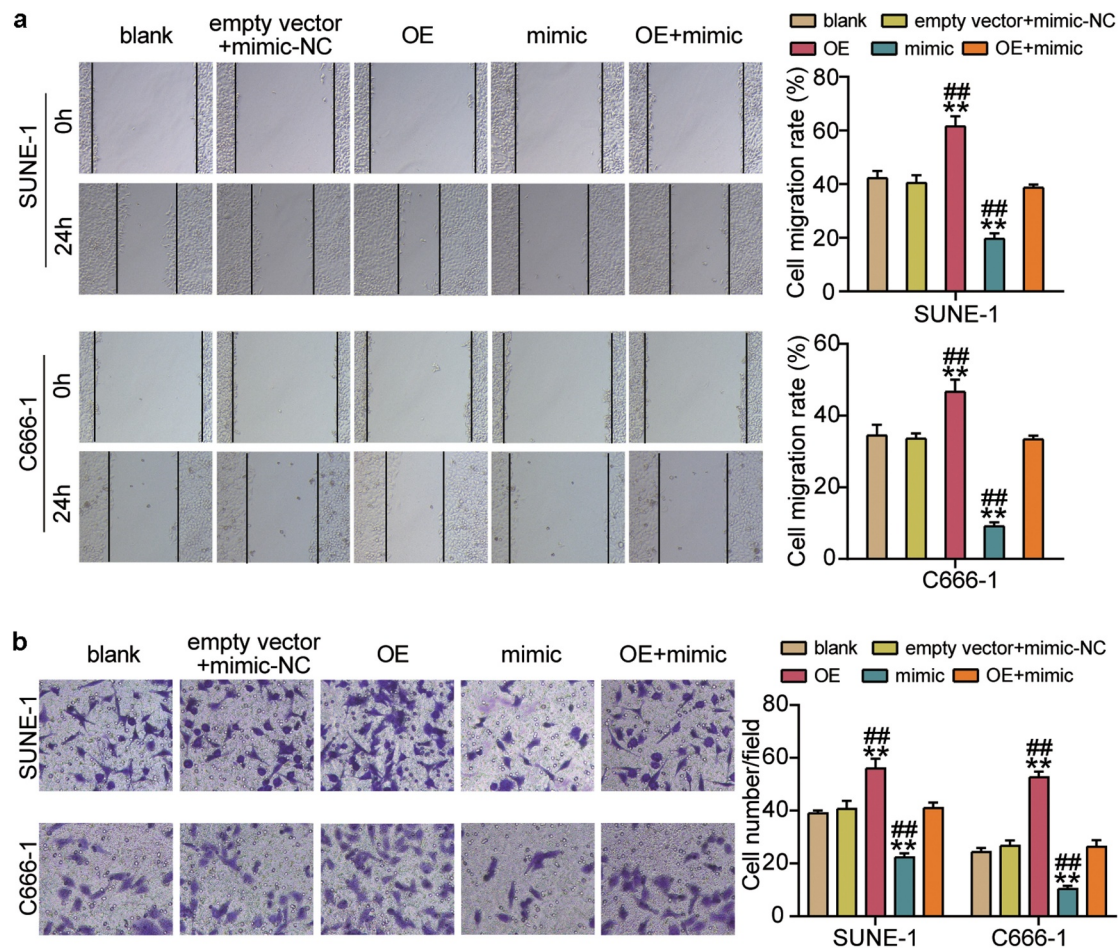


Figure 6. Hsa-miR-150-5p targeting PYCR1 suppressed cell migration and invasion of NPC cells.

(a) Cell migration was detected in C666-1 and SUNE-1 cells transfected with empty vector+mimic-NC, OE, mimic, and mimic+ OE by BrdU assay. (b) Cell invasion was determined in C666-1 and SUNE-1 cells transfected with empty vector+mimic-NC, OE, mimic, and mimic+ OE. $n = 3$. *, $P < 0.05$; **, $P < 0.001$ compared with blank. #, $P < 0.05$; ##, $P < 0.001$ compared with mimic+ OE. NC, negative control; mimic, hsa-miR-150-5p mimic; OE, PYCR1 overexpression; mimic+ OE, hsa-miR-150-5p mimic+ PYCR1 overexpression.

suppressed the expression of *PYCR1*, which inhibited cell growth, migration, and invasion in NPC.

Over the years multiple studies have emphasized the biological role of hsa-miR-150-5p in carcinogenesis [30–32]. Zhou et al. reported that hsa-miR-150-5p was repressed by long non-coding RNA Myocardial Infarction Associated Transcript (lncRNA MIAT), and cell growth was increased by hsa-miR-150-5p mimics, and reversed by the overexpression of MIAT levels [30]. Tian et al. suggested that hsa-miR-150-5p significantly repressed the Wnt/ β -catenin signaling pathway to hamper the stem cell-like characteristics of glioma cells [31]. Lou et al. reported that hsa-miR-150-5p was

inhibited by lncRNA PART1, and the upregulation of hsa-miR-150-5p could prevent the oncogenesis of lncRNA PART1 by inhibiting *LRG1* expression [32]. Liu et al. found that hsa-miR-150-5p directly targeted the kinesin family member 3 C (*KIF3C*) gene to repress its expression and acts as a tumor suppressor in non-small cell lung cancer (NSCLC) progression [33]. Notably, Li et al. revealed that hsa-miR-150-5p reduced cell proliferation and tumorigenesis by arresting the G1/S phase transition in NPC cells [13]. Chan et al. suggested that the Wnt modulator ICG-001 repressed cell growth by decreasing hsa-miR-150-5p levels and upregulating CD44 levels in NPC [11]. However, the

upregulation of hsa-miR-150-5p promotes radioresistance of NPC cells by downregulating *GSK3 β* expression [12]. Our study demonstrated that the hsa-miR-150-5p levels were dramatically downregulated in NPC cells. Furthermore, the upregulation of hsa-miR-150-5p attenuated the growth, migration, and invasion of NPC cells. Moreover, the overexpression of *PYCR1* significantly inhibited the tumor suppressor effect of hsa-miR-150-5p on NPC.

Accumulating evidence has shown that *PYCR1* exerts tumorigenic effects in a variety of cancers [27–29,34,35]. Sun et al. found that *PYCR1* was upregulated by lncRNA TRPM2-AS, which sponges miR-140-3p, significantly promotes the growth of breast cancer cells [34]. Xiao et al. found that the overexpression of *PYCR1* significantly accelerated gastric cancer progression, and patients with high *PYCR1* expression had poor survival outcomes [29]. In addition, *PYCR1* markedly facilitates the migration and invasion of NSCLC cells [35]. Furthermore, silencing of *PYCR1* reduces the cell growth, drug resistance, and epithelial-mesenchymal transition (EMT) by inactivating the p38 mitogen-activated protein kinase (MAPK) and NF- κ B signaling pathways in colorectal cancer cells [27]. The downregulation of *PYCR1* dramatically repressed cell growth and survival by inactivating the c-Jun N-terminal kinase/insulin receptor substrate 1 (JNK/IRS1) pathway in hepatocellular cancer cells [28]. However, the role of *PYCR1* in NPC development remains unclear. In our study, we demonstrated for the first time that *PYCR1* expression is conspicuously upregulated in NPC tissues and cells. The overexpression of *PYCR1* accelerated the growth, migration, and invasion of NPC cells. Importantly, we found that hsa-miR-150-5p suppressed the effect of *PYCR1*, which further suppressed NPC cell progression.

As previously, evidences have revealed that *PYCR1* dramatically enhanced cell growth and survival through activating JNK/IRS1 pathway in the development of hepatocellular cancer [28]. *PYCR1* facilitated cell growth, drug resistance and EMT through activating p38 MAPK and NF- κ B signaling pathways of colorectal cancer cells [27]. However, potential signaling pathways involved in hsa-miR-150-5p-*PYCR1* axis in NPC

needs further elucidation. In addition, the lack of prognostic analysis of NPC patients and in vivo experiments limit the persuasive power of this study to some extent. In the future, we will further explore the correlation between hsa-miR-150-5p-*PYCR1* and patient survival and its effect on NPC tumor growth in vivo.

Conclusions

This study revealed that hsa-miR-150-5p attenuated NPC tumorigenesis by reducing *PYCR1* expression. Therefore, our study provides a comprehensive investigation of hsa-miR-150-5p and *PYCR1* in NPC, which could provide a good potential therapeutic approach for treating patients with NPC.

Availability of data and materials

The datasets used and analyzed during the current study are available from the corresponding author on reasonable request.

List of abbreviations

miRNAs: MicroRNAs; NC: negative control; NSCC: non-small-cell lung cancer; OE: over expression; OSCC: oral squamous cell carcinoma; *PYCR1*: pyrroline-5-carboxylate reductase 1; UTRs: untranslated regions; WT: wild-type.

Disclosure statement

No potential conflict of interest was reported by the authors.

Funding

Hainan Provincial Science Foundation [Grant No.20A200331] provided financial support for the conduct of this work.

Ethics approval and consent to participate

The present study was approved by the Ethics Committee of the First Affiliated Hospital of Hainan Medical University (Haikou, China). The processing of clinical tissue samples is in strict compliance with the ethical standards of the Declaration of Helsinki. All patients signed written informed consent.

Consent for publication

Consent for publication was obtained from the participants.

Authors' contributions

JJH and ZCX conducted the study, collected and analyzed the data. ZQL and XLZ designed the study and methods and collected the funds. CLX analyzed and interpreted the data. JWY collected materials and resources, conducted literature analysis and prepared manuscript. XJZ conducted literature analysis and prepared the manuscript. All authors read and approved the final manuscript.

References

- [1] Jemal A, Bray F, Center MM, et al. Global cancer statistics. *CA Cancer J Clin.* **2011**;61(2):69–90.
- [2] Qu C, Liang Z, Huang J, et al. MiR-205 determines the radioresistance of human nasopharyngeal carcinoma by directly targeting PTEN. *Cell Cycle (Georgetown, Tex).* **2012**;11(4):785–796.
- [3] Ai MD, Li LL, Zhao XR, et al. Regulation of survivin and CDK4 by Epstein-Barr virus encoded latent membrane protein 1 in nasopharyngeal carcinoma cell lines. *Cell Res.* **2005**;15(10):777–784.
- [4] Zhen Y, Fang W, Zhao M, et al. miR-374a-CCND1-pPI3K/AKT-c-JUN feedback loop modulated by PDCC4 suppresses cell growth, metastasis, and sensitizes nasopharyngeal carcinoma to cisplatin. *Oncogene.* **2017**;36(2):275–285.
- [5] Chen L, Song J, Cui J, et al. microRNAs regulate adipocyte differentiation. *Cell Biol Int.* **2013**;37(6):533–546.
- [6] Li X-T, Wang H-Z, Wu Z-W, et al. miR-494-3p regulates cellular proliferation, invasion, migration, and apoptosis by PTEN/AKT signaling in human glioblastoma cells. *Cell Mol Neurobiol.* **2015**;35(5):679–687.
- [7] Chae D-K, Park J, Cho M, et al. MiR-195 and miR-497 suppress tumorigenesis in lung cancer by inhibiting SMURF2-induced TGF- β receptor I ubiquitination. *Mol Oncol.* **2019**;13(12):679–687.
- [8] Jia H, Wu D, Zhang Z, et al. Regulatory effect of the MAFG-AS1/miR-150-5p/MYB axis on the proliferation and migration of breast cancer cells. *Int J Oncol.* **2020**;58(1):33–44.
- [9] Meng X, Sun W, Yu J, et al. LINC00460-miR-149-5p/miR-150-5p-Mutant p53 feedback loop promotes oxaliplatin resistance in colorectal cancer. *Mol Ther Nucleic Acids.* **2020**;22:1004–1015.
- [10] Li X, Ren H. Long noncoding RNA PVT1 promotes tumor cell proliferation, invasion, migration and inhibits apoptosis in oral squamous cell carcinoma by regulating miR-150-5p/GLUT-1. *Oncol Rep.* **2020**;44(4):1524–1538.
- [11] Chan LS, Man OY, Kwok HH, et al. The Wnt modulator ICG-001 mediates the inhibition of nasopharyngeal carcinoma cell migration in vitro via the miR-150/CD44 axis. *Int J Oncol.* **2019**;54(3):1010–1020.
- [12] Huang Y, Tan D, Xiao J, et al. miR-150 contributes to the radioresistance in nasopharyngeal carcinoma cells by targeting glycogen synthase kinase-3 β . *J Cancer Res Ther.* **2018**;14(1):111–118.
- [13] Li X, Liu F, Lin B, et al. miR-150 inhibits proliferation and tumorigenicity via retarding G1/S phase transition in nasopharyngeal carcinoma. *Int J Oncol.* **2017**;50(4):1097–1108.
- [14] Zhu L, Liu Y, Yang Y, et al. CircRNA ZNF609 promotes growth and metastasis of nasopharyngeal carcinoma by competing with microRNA-150-5p. *Eur Rev Med Pharmacol Sci.* **2019**;23(7):2817–2826.
- [15] Gao Y, Luo L, Xie Y, et al. PYCR1 knockdown inhibits the proliferation, migration, and invasion by affecting JAK/STAT signaling pathway in lung adenocarcinoma. *Mol Carcinog.* **2020**;59(5):503–511.
- [16] Wang D, Wang L, Zhang Y, et al. PYCR1 promotes the progression of non-small-cell lung cancer under the negative regulation of miR-488. *Biomed Pharmacother.* **2019**;111:588–595.
- [17] Zeng T, Zhu L, Liao M, et al. Knockdown of PYCR1 inhibits cell proliferation and colony formation via cell cycle arrest and apoptosis in prostate cancer. *Med Oncol.* **2017**;34(2):27.
- [18] Livak KJ, Schmittgen TD. Analysis of relative gene expression data using real-time quantitative PCR and the 2(-Delta Delta C(T)) Method. *Methods.* **2001**;25(4):402–408.
- [19] Huang Y, Yan Q, Yu D, et al. Long intergenic non-protein coding RNA 960 regulates cancer cell viability, migration and invasion through modulating miR-146a-5p/interleukin 1 receptor associated kinase 1 axis in pancreatic ductal adenocarcinoma. *Bioengineered.* **2021**;12(1):369–381.
- [20] Zhao J-T, Chi B-J, Sun Y, et al. LINC00174 is an oncogenic lncRNA of hepatocellular carcinoma and regulates miR-320/S100A10 axis. *Cell Biochem Funct.* **2020**;38(7):859–869.
- [21] Feng J, Li J, Qie P, et al. Long non-coding RNA (lncRNA) PGM5P4-AS1 inhibits lung cancer progression by up-regulating leucine zipper tumor suppressor (LZTS3) through sponging microRNA miR-1275. *Bioengineered.* **2021**;12(1):196–207.
- [22] Cheng J, Lou Y, Jiang K. Downregulation of long non-coding RNA LINC00460 inhibits the proliferation, migration and invasion, and promotes apoptosis of pancreatic cancer cells via modulation of the miR-320b/ARF1 axis. *Bioengineered.* **2021**;12(1):96–107.
- [23] Zhang H, Liu S, Tang L, et al. Long non-coding RNA (lncRNA) MRPL23-AS1 promotes tumor progression and carcinogenesis in osteosarcoma by activating Wnt/

- β -catenin signaling via inhibiting microRNA miR-30b and upregulating myosin heavy chain 9 (MYH9). *Bioengineered*. 2021;12(1):162–171.
- [24] Awan HM, Shah A, Rashid F, et al. Comparing two approaches of miR-34a target identification, biotinylated-miRNA pulldown vs miRNA overexpression. *RNA Biol*. 2018;15(1):55–61.
- [25] Wang X, Wang J. High-content hydrogen water-induced downregulation of miR-136 alleviates non-alcoholic fatty liver disease by regulating Nrf2 via targeting MEG3. *Biol Chem*. 2018;399(4):397–406.
- [26] Wang G, Bai X, Jiang G, et al. GIT1 overexpression promotes epithelial-mesenchymal transition and predicts poor prognosis in hepatocellular carcinoma. *Bioengineered*. 2021;12(1):30–43.
- [27] Yan K, Xu X, Wu T, et al. Knockdown of PYCR1 inhibits proliferation, drug resistance and EMT in colorectal cancer cells by regulating STAT3-Mediated p38 MAPK and NF- κ B signalling pathway. *Biochem Biophys Res Commun*. 2019;520(2):486–491.
- [28] Zhuang J, Song Y, Ye Y, et al. PYCR1 interference inhibits cell growth and survival via c-Jun N-terminal kinase/insulin receptor substrate 1 (JNK/IRS1) pathway in hepatocellular cancer. *J Transl Med*. 2019;17(1):343.
- [29] Xiao S, Li S, Yuan Z, et al. Pyrroline-5-carboxylate reductase 1 (PYCR1) upregulation contributes to gastric cancer progression and indicates poor survival outcome. *Ann Transl Med*. 2020;8(15):937.
- [30] Zhou S, Xu A, Song T, et al. lncRNA MIAT regulates cell growth, migration, and invasion through sponging miR-150-5p in ovarian cancer. *Cancer Biother Radiopharm*. 2020;35(9):650–660.
- [31] Tian W, Zhu W, Jiang J. miR-150-5p suppresses the stem cell-like characteristics of glioma cells by targeting the Wnt/ β -catenin signaling pathway. *Cell Biol Int*. 2020;44(5):1156–1167.
- [32] Lou T, Ke K, Zhang L, et al. PART1 facilitates the malignant progression of colorectal cancer via miR-150-5p/LRG1 axis. *J Cell Biochem*. 2020;121(10):4271–4281.
- [33] Liu H, Liu R, Hao M, et al. Kinesin family member 3C (KIF3C) is a novel non-small cell lung cancer (NSCLC) oncogene whose expression is modulated by microRNA-150-5p (miR-150-5p) and microRNA-186-3p (miR-186-3p). *Bioengineered*. 2021;12(1):3077–3088.
- [34] Sun T, Song Y, Yu H, et al. Identification of lncRNA TRPM2-AS/miR-140-3p/PYCR1 axis's proliferates and anti-apoptotic effect on breast cancer using co-expression network analysis. *Cancer Biol Ther*. 2019;20(6):4271–4281.
- [35] Sang S, Zhang C, Shan J. Pyrroline-5-carboxylate reductase 1 accelerates the migration and invasion of nonsmall cell lung cancer in vitro. *Cancer Biother Radiopharm*. 2019;34(6):380–387.